Adsorption of NO on Cu Exchanged Zeolites, an FTIR Study: Effects of Cu Levels, NO Pressure, and Catalyst Pretreatment

T. Cheung,* S. K. Bhargava,* M. Hobday,* and K. Foger†,[1]

*Department of Applied Chemistry, Royal Melbourne Institute of Technology, GPO Box 2476V, Melbourne, Victoria 3001, Australia; and †CSIRO Division of Materials Science and Technology, Private Bag 33, Rosebank MDC, Clayton, Victoria 3168, Australia

Three different copper zeolite systems (Cu–ZSM5, Cu–UHSY, and Cu–mordenite) have been prepared with different copper loadings from low to over exchange levels. The surface chemistry of three systems has been studied using IR spectra of adsorbed NO. Most of the copper in Cu–ZSM5 was in the form of Cu(I). Cu(II) species were predominant in Cu–mordenite. For Cu–UHSY the number of Cu(I) species increased as the level of copper loading increased. The catalytic activity for NO decomposition appeared to depend on a Cu(I)–Cu(II) redox cycle which resulted in the formation of an ON–Cu^{2+}–NO$_2^-$ complex, previously postulated as the critical intermediate in the reaction. Both oxidation and regeneration of the Cu(I) sites in Cu–ZSM5 occurred readily. In Cu–UHSY oxidation was low, suggesting that Cu(I) species were more stable. Cu(II) was the prominent copper species in Cu–mordenite, and regeneration of the Cu(I) sites was difficult. Stability, oxidation, and regeneration of Cu(I) sites play a major role in NO decomposition. In over-exchanged Cu–ZSM5, the Cu(I) sites were more stable, and the rate of oxidation was high. Furthermore a large number of reduced sites were readily regenerated from the Cu(II), thus making it the most effective catalyst for the decomposition of NO. © 1996 Academic Press, Inc.

1. INTRODUCTION

Eliminating emissions of nitrogen oxides (NO$_x$) from the atmosphere is an important issue in atmospheric pollution control. Nitrogen oxides emitted from mobile and stationery sources pose a substantial environmental hazard. NO$_x$ when combined with other air pollutants such as SO$_2$ and volatile organic compounds contribute to acid rain and photochemical smog (1–2).

In automotive pollution control the removal of NO$_x$ is achieved with the "three-way" catalytic converter (3). However, the recent drive to "lean burn" engines in order to achieve higher fuel efficiency as well as diesel engine emission laws require the development of new technology

for NO$_x$ control (3). Selective catalytic reduction (SCR) with ammonia as reducing agent is the most common technology for NO$_x$ control in stationary installations, e.g., power stations. However, direct decomposition of NO$_x$ into its constituents, N$_2$ and O$_2$ (Eq. [1]), without using a reducing agent appears to be a very attractive option.

$$2NO \xrightarrow{\text{catalyst}} N_2 + O_2 \dots \qquad [1]$$
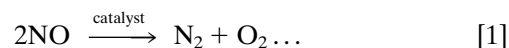
This decomposition (Eq. [1]) is thermodynamically favorable but kinetically hindered, and is therefore only achieved with a catalyst. To date no catalyst has shown sufficient activity for a practical process (4–8). O$_2$ contained in the feed gas or released by the decomposition of NO competes with NO for the absorption sites. However, Cu–ZSM5, the best catalyst reported, desorbs O$_2$ at high temperature (823 K) restoring its catalytic activity (9–11). The unique nature of this system is that "over-exchanged" Cu–ZSM5 can deliver reasonable NO reduction activity and durability. According to Iwamoto *et al.* (11) the excess copper participates in the reduction reaction, as evidenced by the finding that 94% of Cu(II) ions exchanged into Cu–ZSM5 were active for NO adsorption.

The mechanism of the decomposition of NO has been studied by Li and Armor (12), Iwamoto *et al.* (13–14), Li and Hall (15–16), Spoto *et al.* (17–18), Ebitani *et al.* (19), Valyon and Hall (20–21), and Giamello *et al.* (22).

A recent report by Spoto *et al.* (17) gives a detailed account of the interaction of NO with Cu(I)–ZSM5. Unlike previous investigations, a Cu–ZSM5 catalyst was prepared which contained exclusively Cu(I) ions in the framework. From the findings a reaction scheme was proposed which agreed with the work by Giamello *et al.* (22).

In this work the surface interaction between NO and Cu exchanged zeolites has been examined by FTIR to determine in detail the role of over-exchanged Cu–ZSM5 and of Cu ions in different zeolite matrices such as UHSY and mordenite.

---

[1] To whom correspondence should be addressed.

2. EXPERIMENTAL

2.1. Catalysts

Copper was exchanged into ZSM5, UHSY, and mordenite by ion-exchange with a Cu–nitrate solution, according to the method described by Iwamoto et al. (11). The copper content was determined by AAS and exchange levels were calculated based on the assumption that one Cu(II) replaced two Na ions. Sample identifiers contain the metal cation, zeolite type, and the level of exchange (e.g., Cu–ZSM5-68).

2.2. FTIR Measurements

Measurements were carried out in an *in situ* cell. A self supporting wafer of 1.5 cm in diameter was pressed and was fixed to a stainless steel holder located in the sample holder of a Pyrex/quartz cell.

Spectra were recorded at room temperature on a computer-controlled Mattson Cygnus 100 spectrometer, equipped with an MCT detector. The spectrum of the dehydrated sample was used as a background from which the adsorbed spectrum was subtracted.

2.3. Procedures

Prior to recording of spectra, the wafer was heated at 3° C/min to 300°C for 3 hr, at a pressure $<10^{-3}$ Torr to remove atmospheric O_2, CO_2, and moisture. This sample was designated *dehydrated* catalyst.

The *reduced* or *oxidized* form was obtained by heating the wafer under flowing 5% H_2/N_2 or 1% O_2/N_2 at 300°C for 1 hr, respectively.

NO was passed through a dry ice trap before contacting the wafer at room temperature. Incremental dosages were admitted and spectra were recorded after each dose.

3. RESULTS

3.1. Assignment of IR Bands

This work and previous studies (14, 17, 21, 22, 26–27) of NO adsorption on Cu–ZSM5, Cu–UHSY, and Cu–mordenite catalysts with NO have suggested that NO coordinates either to Cu(II) or Cu(I) but not to Cu–metal. This was verified with Cu in SiO_2 which exists either as Cu(II) or Cu–metal since Cu(I) is not stable on the silica support. When the reduced form of a Cu/SiO_2 wafer which consisted of Cu–metal was exposed to NO, IR peaks of adsorbed NO were not observed even at an NO pressure of 24 Torr.

The interaction between NO and Cu–ZSM5 always resulted in the formation of three major nitrosyl complexes [Cu^{2+}–NO, Cu^+–NO, and Cu^+–$(NO)_2$]. For example, Fig. 1 shows a spectrum of dehydrated Cu—ZSM5 (fully Cu exchanged) after the addition of 20 Torr of NO. Bands at 1900, 1810, 1824, and 1730 cm^{-1} were apparent. The bands at 1824 and 1730 cm^{-1} have been assigned as the symmetric
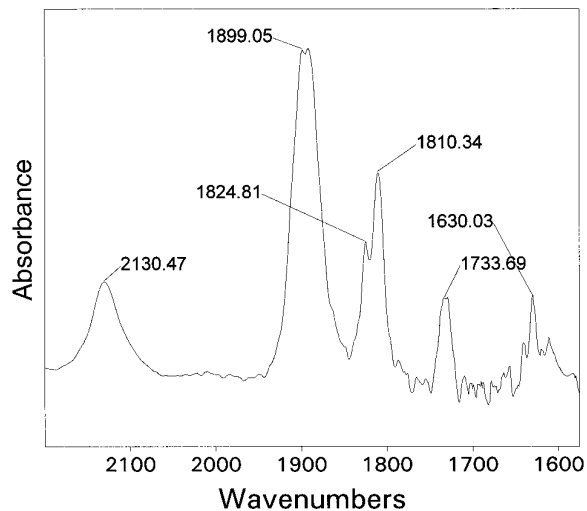

FIG. 1. Dehydrated Cu–ZSM5-103, P_{NO} = 20 Torr.

dinitrosyl band (1824 cm^{-1}) and the asymmetric dinitrosyl band (1730 cm^{-1}) by Spoto et al. (17, 18) and by Valyon Hall (21) with tracer experiments using a mixture of ^{15}NO and ^{14}NO. Similar assignments have been made by Iwamoto et al. (13) and Guillory and Hunter (24). A band at 2130 cm^{-1} was also apparent which was assigned to N_2O. The 1810 cm^{-1} band was assigned to the Cu^+–NO species.

To assign the 1900 cm^{-1} band, a fully oxidized Cu–ZSM5 wafer, which would contain Cu^{2+} ions only, was exposed to NO. As expected, the dominant band appeared at 1900 cm^{-1}, which was thus assigned to Cu^{2+}–NO species.

The nitrosyl copper complexes and intermediates resulting from surface reaction between NO and Cu–zeolites are summarized in Table 1. The position and intensity of these IR bands depended on NO pressure, copper content, zeolite support, and pretreatment.

3.2. Adsorption of NO onto Cu–Zeolite Catalysts: Effects of Pretreatments and Copper Levels

3.2.1. Dehydrated Cu–ZSM5. The FTIR results are summarized in Figs. 2, 3, and 4. For all Cu exchange levels,

TABLE 1

Infrared Bands of Species Resulting from the Adsorption of NO with Cu–Zeolite

Species	Cu–ZSM5	Cu–UHSY	Cu–mordenite
Cu(I)–NO	1810	1815–1819	1807–1810
Cu(II)–NO	1900–1910	1898–1900	1905–1910
	—	1950	1950
Cu(I)–$(NO)_2$ (sym)	1824	—	—
Cu(I)–$(NO)_2$ (asym)	1727–1738	1730–1740	1736–1738
Cu(II)–NO_2	1600–1630	1600–1630	1600–1630
N_2O ads	2130	2250–2150	2250–2150

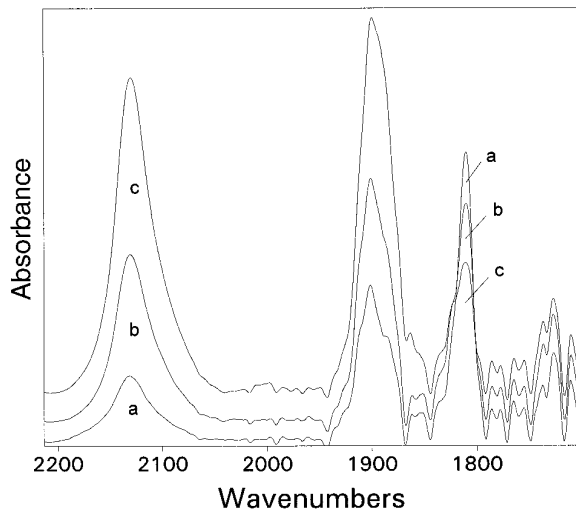**FIG. 2.** Dehydrated Cu–ZSM5-68, a = 6 Torr, b = 12 Torr, c = 21 Torr.

FIG. 4. Dehydrated Cu–ZSM5-158, a = 4 Torr, b = 16 Torr.

the dominant band at low NO pressures was observed at 1810 cm^{-1}. In addition smaller bands were present at 1900, 2130, and 1730 cm^{-1}. The strong 1810-cm^{-1} band suggested that the predominant Cu species was Cu(I). With increasing NO dosage the 1900-cm^{-1} band increased, and the 1810-cm^{-1} band decreased. At NO pressures in the range 21–24 Torr the 1900-cm^{-1} band became dominant. In parallel with the 1900-cm^{-1} band a band at 2130-cm^{-1} appeared. This band was assigned to N_2O, formed by oxidation of Cu(I)–NO to Cu(II) (see scheme outlined in Fig. 23), followed by the release of N_2O. Thus, the intensity of the N_2O band appears to be a qualitative measure of the ease of oxidation of Cu(I) to Cu(II). The increase in intensity of the 2130-cm^{-1} band was fastest in Cu–ZSM5-68, suggesting that NO rapidly oxidizes Cu(I) to Cu(II). However, the
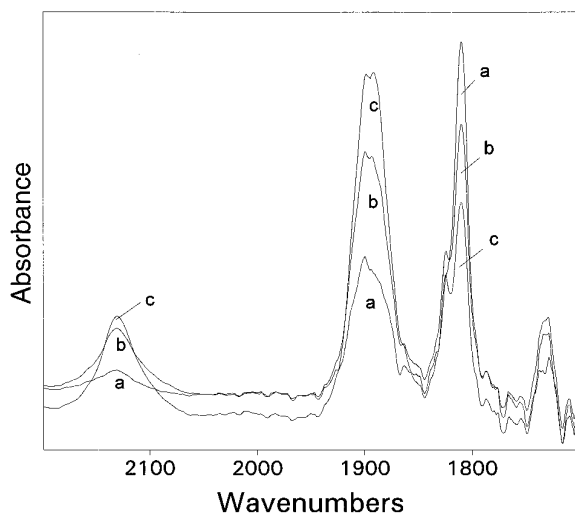
2130-cm^{-1} band grew at a slower rate for Cu–ZSM5-103 and Cu–ZSM5-158, indicating that the Cu(I) was more stable in high (Cu–ZSM5-103) and over-exchanged (Cu–ZSM5-158) Cu–ZSM5.

The asymmetric dinitrosyl band (1730 cm^{-1}) formed at low NO partial pressures (2 Torr) and then grew in intensity as the 1810-cm^{-1} band decreased, as a result of the conversion of the mononitrosyl to the dinitrosyl species. At even higher NO pressure, the band started to decrease. The formation of the symmetric band of the dinitrosyl species at 1824 cm^{-1} was only found in Cu–ZSM5-103 (p_{NO} = 13 Torr) and Cu–ZSM5-158 (p_{NO} = 16 Torr) (see Figs. 3 and 4).

Evacuation of gas phase NO at room temperature (RT) for 30 min lowered the intensity of all three major IR bands (at 2130, 1900, and 1810 cm^{-1}), while a band at 1630 cm^{-1}, characteristic of nitrate species, became more intense (Fig. 5). After evacuation all IR peaks, except the 1900 and 1630 cm^{-1} bands, were removed in Cu–ZSM5-68, and the 1600 cm^{-1} became more intense after evacuation. With increasing Cu-content of the zeolite the three bands were more difficult to remove, an indication that NO was more strongly sorbed to the surface.

3.2.2. Oxidized Cu-ZSM5. Treatment of the catalysts with 1% O_2 in He at 300°C and cooling in this atmosphere prior to adsorption of NO resulted in the spectra shown in Figs. 6, 7, and 8. The strongest IR band appeared at 1900 cm^{-1}, as expected for a Cu(II)–NO complex. A weak 1810 cm^{-1} band indicated that a small number of Cu(I) species still remained.

After desorption and readsorption of NO, all bands were restored, as evacuation resulted in partial reduction of Cu(II) to Cu(I). A comparison of the intensity ratio of the IR peaks at 1900 and 1810 cm^{-1} at low NO partial pressure suggested that the ease of reduction of Cu(II) to Cu(I)
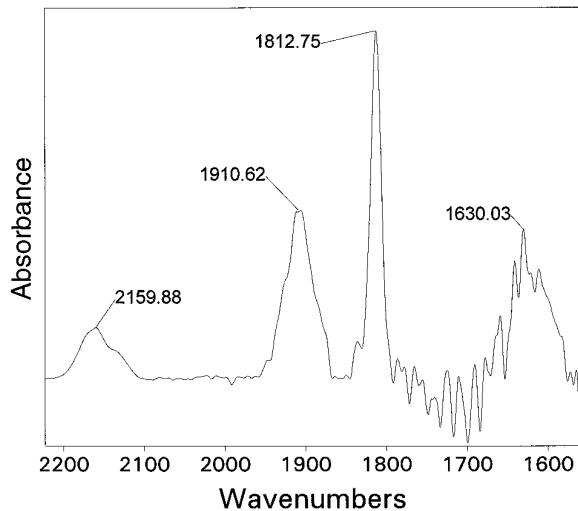

FIG. 3. Dehydrated Cu–ZSM5-103, a = 6 Torr, b = 13 Torr, c = 20 Torr.

FIG. 5. Dehydrated Cu–ZSM5-158, evacuated at RT for 30 min.

FIG. 7. Oxidized Cu–ZSM5-103, a = 4 Torr, b = 18 Torr.

during evacuation followed the series Cu–ZSM5-68 < Cu–ZSM5-103 < Cu–ZSM5-158. More Cu(I) sites are created in zeolites with higher Cu levels. Similar to the dehydrated catalyst, evacuation at RT for 1 hr removed the 1810 cm^{-1} band for Cu–ZSM5-68 and Cu–ZSM5-103, but not for Cu–ZSM5-158 which is in agreement with the assumption that Cu(I) is more stable in over-exchanged ZSM5.

3.2.3. Reduced Cu–ZSM5. After treatment of the wafer in CO or 5% H$_2$/N$_2$, Cu ions in ZSM5 were converted to Cu(I) species, as indicated by the very intense 1810-cm^{-1} band (Figs. 9, 10, and 11). With increasing NO partial pressure the 1810-cm^{-1} band decreased in intensity, while the 1900-cm^{-1} band increased. The decrease of the 1810-cm^{-1} band was a result of the formation of the dinitrosyl species to give an IR band at 1730 cm^{-1}. At higher NO
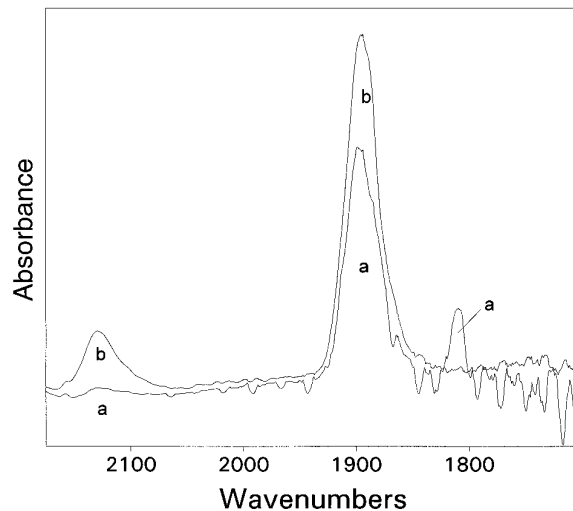
pressures the Cu(I)–dinitrosyl complex is oxidized to a Cu(II) species and N$_2$O. In samples with high Cu exchange (ZSM5-103, ZSM5-158) a higher NO pressure is required for oxidation. For example, the 1730-cm^{-1} band decreased at NO partial pressures of 15, 20, and 24 Torr for Cu–ZSM5-68, Cu–ZSM5-103, and Cu–ZSM5-158, respectively. The asymmetric dinitrosyl band (1824 cm^{-1}) was not observed in Cu–ZSM5-68 but was found in the other two samples at 15 Torr.

Desorption of NO by evacuation led to the reduction of Cu(II) sites to Cu(I) as demonstrated by the appearance of the 1810-cm^{-1} band after readsorption of NO (Fig. 12). Subsequent evacuation did not remove the adsorbed species giving rise to the IR bands at 1900 and 1810 cm^{-1} in Cu–ZSM5-158, whereas they were removed in Cu–ZSM5-68 and Cu–ZSM5-103.
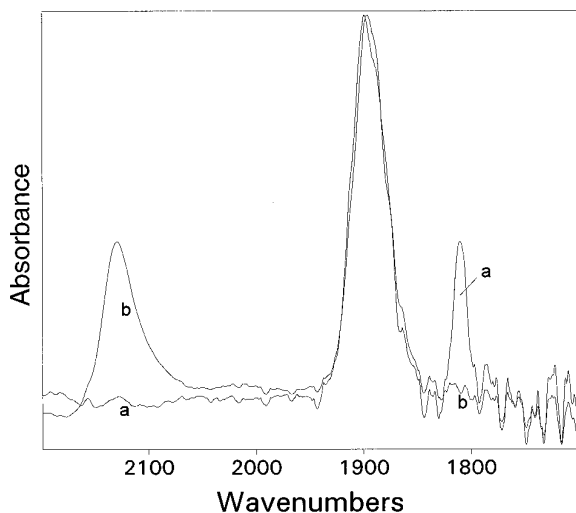

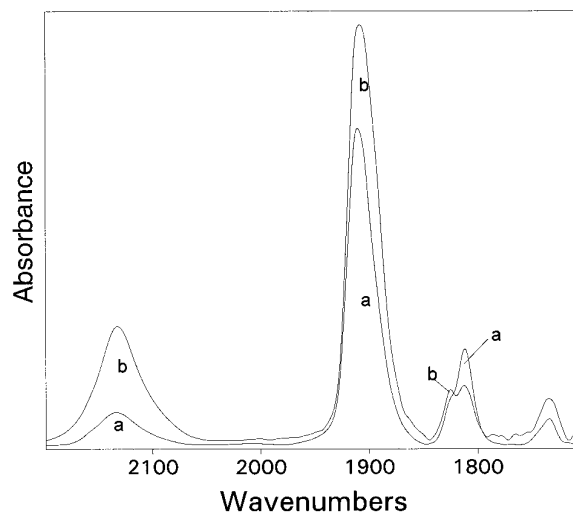**FIG. 6.** Oxidized Cu–ZSM5-68, a = 3 Torr, b = 20 Torr.

FIG. 8. Oxidized Cu—ZSM5-158, a = 6 Torr, b = 26 Torr.

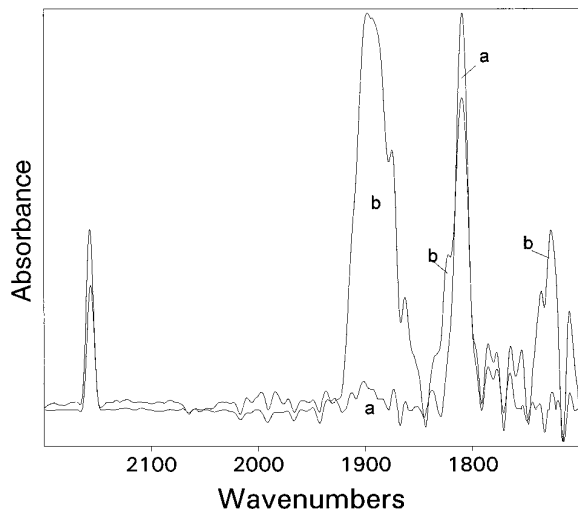**FIG. 9.** Reduced Cu–ZSM5-68, a = 2 Torr, b = 15 Torr.

FIG. 11. Reduced Cu–ZSM5-158, a = 2 Torr, b = 24 Torr.

3.2.4. Dehydrated Cu–UHSY. Three princpal IR bands were observed at 1950, at 1900 and at 1815 cm^{-1}, when NO adsorbed onto dehydrated Cu–UHSY. Both IR bands at 1950 and 1900 cm^{-1} were assigned to NO coordinated to Cu^{2+} ions, but the presence of two peaks suggested that Cu(II) ions in two different locations and chemical environments were present.

In Cu–UHSY-165 the 1815 cm^{-1} IR band was the strongest peak at low NO pressures suggesting that most of the copper was present as Cu(I) species, whereas mostly Cu(II) was apparent in Cu–UHSY-53 (Figs. 13 and 14).

With increasing NO pressure the intensity of the 1815-cm^{-1} band decreased, substantially in Cu–UHSY-53 and to a lesser extent in Cu–UHSY-165 (Fig. 13). The IR band at 1740 cm^{-1} increased as Cu(I) sites from the mononitrosyl species were converted to dinitrosyl species. The 1950-
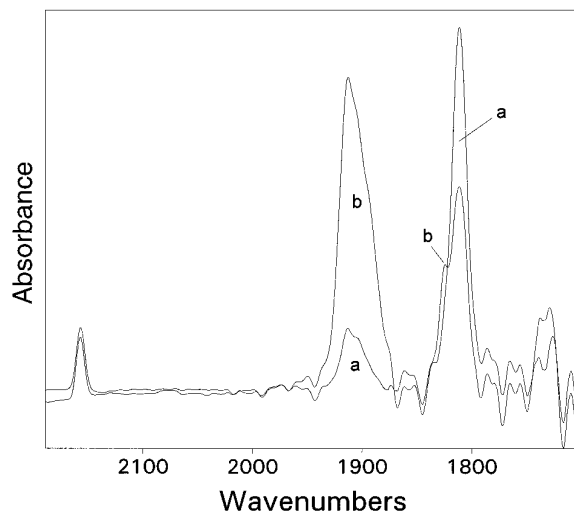
cm^{-1} band was strong in Cu–UHSY-53 and only weak in Cu–UHSY-165, and the peak decreased in intensity with increasing NO pressure. Interconversion of some of the Cu(I) sites to Cu(II) occurred at low pressures with Cu–UHSY-53 while a pressure greater than 13 Torr was necessary for Cu–UHSY-165. Similarly a broad band at 2250–2150 cm^{-1} appeared for Cu–UHSY-53, but it was smaller for Cu–UHSY-165.

Evacuation of both wafers lowered the intensity of all nitrosyl bands with the exception of the 1600-cm^{-1} band which became more intense.

3.2.5. Oxidized Cu–UHSY. Spectra of oxidized Cu–UHSY are shown in Figs. 15 and 16. The 1900-cm^{-1} doublet was the dominant band in Cu–UHSY-53, about 3.5 times more intense than the 1815-cm^{-1} (Fig. 15). For Cu–UHSY-
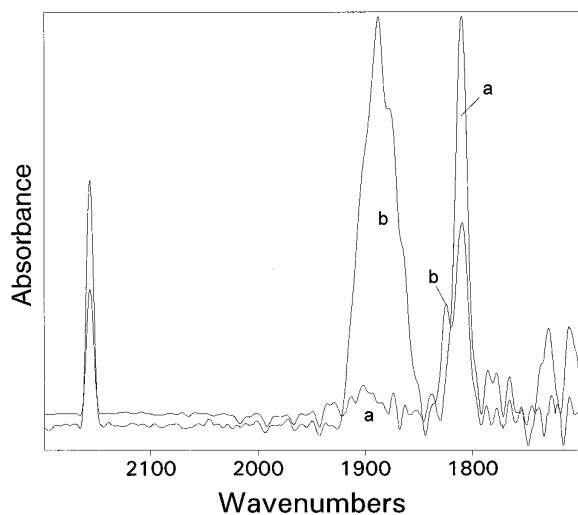

FIG. 10. Reduced Cu–ZSM5-103, a = 2 Torr, b = 20 Torr.
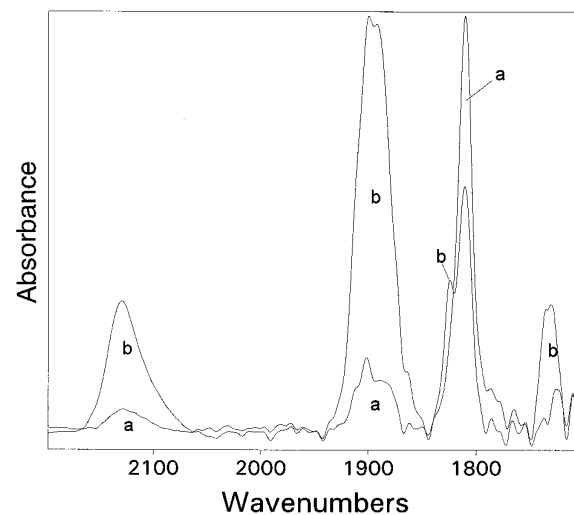

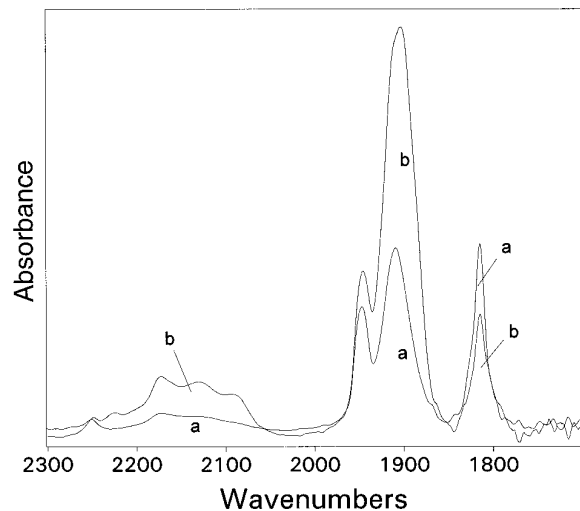**FIG. 12.** Desorbed reduced Cu–ZSM5-103, a = 2 Torr, b = 15 Torr.

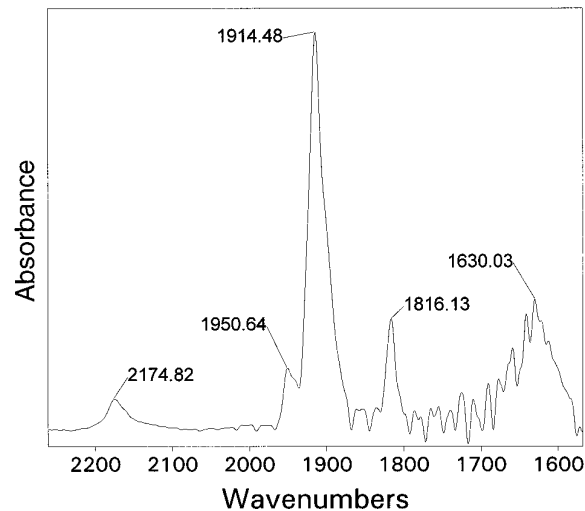FIG. 13.   Dehydrated Cu–UHSY-53, a = 2 Torr, b = 28 Torr.

FIG. 15.   Oxidized Cu–UHSY-53, P_{NO} = 2 Torr.

165 however, both bands were still present and almost equal in intensity at low pressures (Fig. 16). The oxidation treatment as described in Section 2.3 was not effective in oxidizing all Cu ions to Cu(II). The 1815-cm^{-1} band started to decrease at an NO pressure of 13 Torr, and similarly, the 1950-cm^{-1} band also decreased in intensity (Fig. 16).

Evacuation after NO adsorption on the oxidized Cu–UHSY-165 sample regenerated a large number of Cu(I) sites as demonstrated by the dominant 1815-cm^{-1} band after subsequent NO adsorption. It appeared that Cu(I) sites in over-exchanged Cu–UHSY were easily generated however (Figs. 17 and 18).

3.2.6. Reduced Cu–UHSY.   The dominant IR band after NO adsorption of Cu–UHSY reduced in flowing hydrogen at 300° C was at 1815 cm^{-1}, as expected for a Cu(I)–NO complex (Fig. 19).

With increasing NO partial pressure all nitrosyl bands increased in intensity, but the band at 1815 cm^{-1} always dominated. The 1815-cm^{-1} band and the 1900-cm^{-1} band increased. This observation agreed with the finding of Valyon and Hall (21); they observed that all the bands at low pressure appeared with a higher intensity at higher pressure. It appeared that Cu(I) and Cu(II) sites were progressively being filled with NO molecules. The 2150-cm^{-1} band was not observed. The small sharp band at 2165 cm^{-1} can be attributed to adsorbed hydrogen (Fig. 19).

A desorption treatment lowered the intensity of the 1600-cm^{-1} band considerably and removed the H$_2$ band. After addition of NO to this sample a small amount of oxidation was observed as evidenced by the very weak and only very slowly increasing IR band at 2150 cm^{-1} attributed to adsorbed N$_2$O.
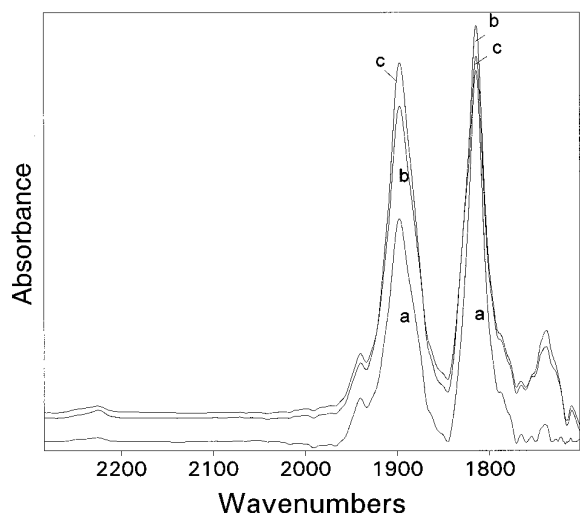

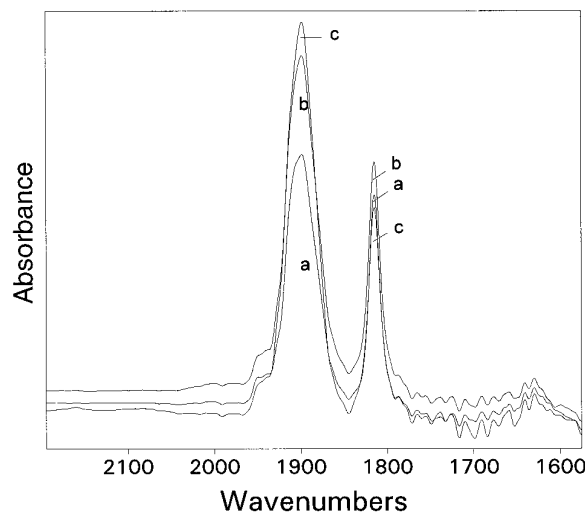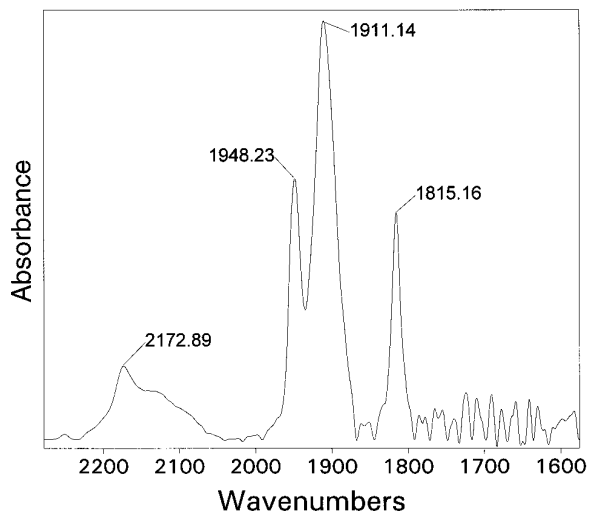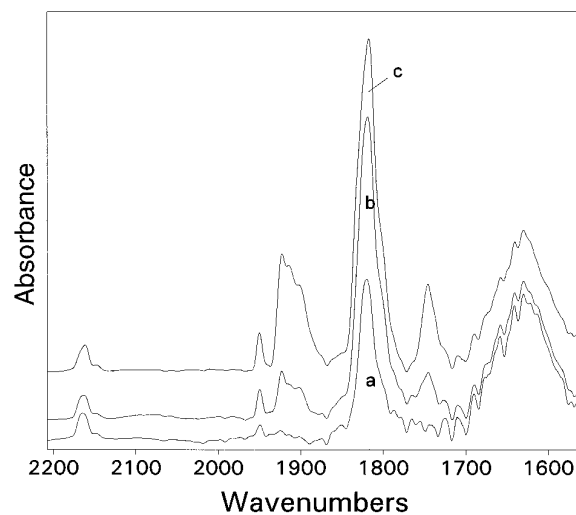FIG. 14.   Dehydrated-165, a = 13 Torr, b = 24 Torr, c = 35 Torr.

FIG. 16.   Oxidized Cu–UHSY-165, a = 2 Torr, b = 6 Torr, c = 13 Torr.

FIG. 17.   Desorbed oxidized Cu–UHSY-53, P_{NO} = 2 Torr.

FIG. 19.   Reduced Cu–UHSY-53, a = 2 Torr, b = 14 Torr, c = 35 Torr.

3.2.7. Dehydrated Cu–mordenite.   The spectra of Cu–mordenite (Cu–M) samples were similar to those obtained in the Cu–UHSY samples. The same nitrosyl species were observed (Table 1) but their behavior with addition of NO differed (Fig. 20).

In both Cu–M-57 and Cu–M-127 the 1900-cm^{-1} band was the dominant peak followed by a smaller 1810-cm^{-1} band. The intensity ratio of the bands at 1900 cm^{-1} and 1810 cm^{-1} was 2. This ratio remained constant until a total pressure of 13–15 Torr was reached indicating filling of Cu(I) and Cu(II) sites. At higher NO pressure the 1810-cm^{-1} band decreased as the mononitrosyl was converted to the dinitrosyl species (appearance of band at 1730 cm^{-1}). The 1900-cm^{-1} band continued to increase in intensity. A weak broad band in the range 2250–2150 cm^{-1} was detected, suggesting some oxidation of Cu(I) to Cu(II).

3.2.8. Oxidized Cu–mordenite.   There was little difference in the spectra of NO adsorbed on Cu–M-127 and on Cu–M-57. The strongest band occurred at 1900 cm^{-1}, and smaller bands occurred at 1810, 2168, and 1620 cm^{-1}. The ratio of the bands at 1900 and 1810 cm^{-1} changed little with increasing NO pressure, but a small dinitrosyl band appeared at 1737 cm^{-1}, and the N_2O peak at 2168 cm^{-1} grew slightly (Fig. 21).

After desorption some of the Cu(II) was reduced to Cu(I), but not to a marked degree. The 1730-cm^{-1} band appeared at a NO pressure of 7 Torr, similar to the oxidized form and did not vary for samples with varying degrees of Cu exchange.

3.2.9. Reduced Cu–mordenite.   No adsorption was observed after H_2 treatment even after admission of 26 Torr of NO. The H_2 treatment appears to inhibit adsorption of
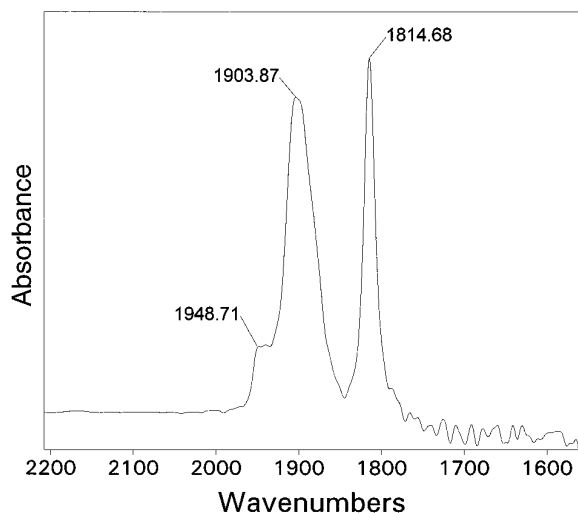
FIG. 18.   Desorbed oxidized Cu–UHSY-165, P_{NO} = 2 Torr.
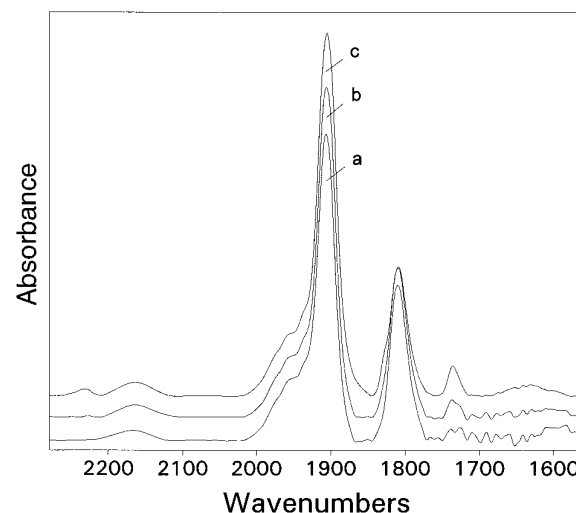
FIG. 20.   Dehydrated Cu–M-127, a = 6 Torr, b = 13 Torr, c = 25 Torr.
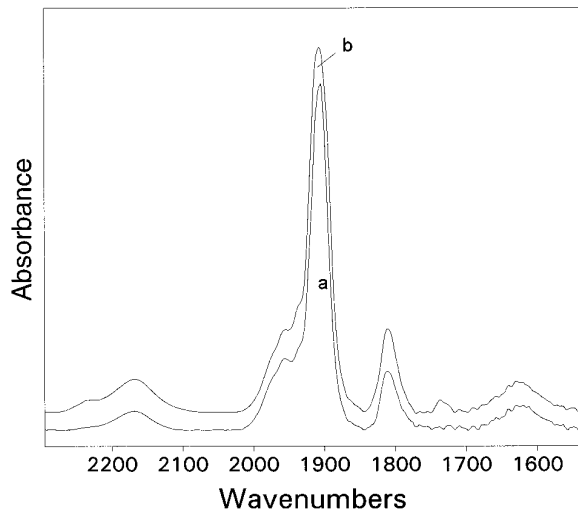
FIG. 21. Oxidized Cu–M-57, a = 2 Torr, b = 14 Torr.

FIG. 23. Mechanism for the decomposition of NO.

NO on copper sites. Only the sharp IR band at 2160–2165 cm^{-1} for adsorbed hydrogen was apparent.

After a desorption the active sites available for NO adsorption were restored. Initially, the Cu(I) band at 1810 cm^{-1} dominated, but at higher NO pressures the 1900-cm^{-1} band increased, but without a noticeable decrease of the 1810-cm^{-1} band. Minor bands at 1730 and 2160 cm^{-1} were apparent (Fig. 22). It appeared that only hydrogen reduction was able to produce significant amounts of Cu(I).

4. DISCUSSION

4.1. Differences Between Different Zeolites and Pretreatments

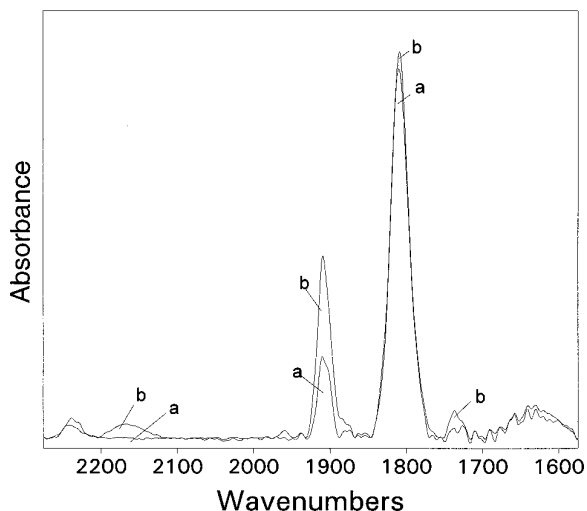*4.1.1. Cu in ZSM-5 matrix.* For most pretreatment conditions, with the exception of oxygen treatment at 300°C

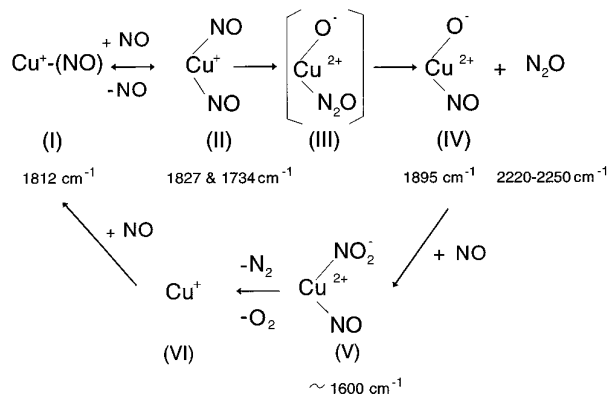**FIG. 22.** Desorbed reduced Cu–M-57, a = 6 Torr, b = 14 Torr.

followed by cooling in oxygen to RT, the Cu^+–NO^- peak is the major species in the Cu–ZSM5 system at low NO partial pressures, but as the NO pressure increases the species is rapidly converted to a Cu^{2+}–NO complex via the scheme outlined in Fig. 23. The intensity of the Cu(I) species is highest for higher degrees of Cu exchange. The ease of oxidation of Cu(I) species by NO follows the order Cu–ZSM5-68 > Cu–ZSM5-103 > Cu–ZSM5-158, as evidenced by the rate of increase of the 2130-cm^{-1} band (N_2O) and the rate of decrease of the 1800-cm^{-1} peak. Furthermore, the dinitrosyl peak first increased with NO pressure but then decreased, e.g., in Cu–ZSM5-158 at 16 Torr NO, for Cu–ZSM5-103 at 13 Torr, and for Cu–ZSM5-68 at 7 Torr. These observations are a clear indication that Cu(I) sites are more stable in Cu–ZSM5-158 than in the other two samples.

Oxidation leads to a decrease in the number of Cu(I) sites available for NO adsorption. To continue the catalytic cycle, Cu(I) sites must be regenerated, which can be achieved with a desorption treatment. This conversion was easiest in Cu–ZSM5-158, while the least number of Cu(I) sites were recovered in Cu–ZSM5-68.

After oxygen treatment followed by desorption at 300°C, NO is especially active for conversion of Cu(I) to Cu(II) via the above reaction scheme, as evidenced by a very strong N_2O peak, a fast decreasing Cu^+–NO peak, and an increasing dinitrosyl peak.

4.1.2. Mordenite. Copper in Cu–mordenite was present as Cu(I) and Cu(II). Both bands increased with increasing NO pressure, until all sites were saturated. However, Cu(II) was more abundant than Cu(I), except after strong reduction treatments in hydrogen or CO. This was supported by a strong 1900-cm^{-1} band particularly in Cu–M-127. NO is more strongly adsorbed on Cu(I) sites as the Cu–NO complex forms first. As the NO pressure increases, Cu^{2+}–NO also forms and eventually saturates.

The ratio Cu(I) to Cu(II) is determined by the pretreatment as interconversion between sites occurs only to a

small extent and only at high NO pressures, as demonstrated by the slight decrease in the Cu^+–NO band at 1800 cm^{-1} associated with a further increase in the Cu^{2+}–NO peak and a weak N_2O band in the region 2150–2250 cm^{-1}. In contrast to the ZSM-5 system, Cu(I) sites are more abundant in Cu–M-57 compared to over-exchanged Cu–M-127. Again, interconversion is easiest after oxygen treatment followed by desorption at 300°C.

4.1.3. UHY. Oxidation of the Cu(I) sites in Cu–UHSY samples was dependent on the level of Cu exchange and the pretreatment. In Cu–UHSY-53 Cu(I) was more readily oxidized to Cu(II) whereas Cu(I) species were more stable in Cu–UHSY-165 as evidenced by the relative ease Cu(II) was reduced to Cu(I) during desorption; furthermore the presence of a substantial number of Cu(I) sites are still present after oxygen treatment at 300°C and cooling in oxygen. Similar to Cu–mordenite interconversion was easier after oxygen pretreatment.

4.2. General

The nature of adsorption of NO onto the surface was influenced by the degree of Cu exchange, pretreatment and choice of zeolite matrix. Copper exchanged into the zeolite framework (ZSM5, UHSY, and mordenite) was present as a mixture of Cu(II) and Cu(I) species. The ratio of Cu(I) to Cu(II) depended on the zeolite type (matrix and location dependent), level of exchange, and pretreatment. Both Cu(I) and Cu(II) species are active sites for NO adsorption. Exposure of NO to the Cu(II) sites resulted in a Cu^{2+}–NO band at 1900 cm^{-1}; for Cu(I) sites a Cu^+–NO^- band at 1810 cm^{-1} appeared. At higher NO pressure the Cu(I) mononitrosyl species transformed into a dinitrosyl species characterized by two IR bands at 1824 cm^{-1} (asymmetric) and 1730 cm^{-1} (symmetric). The N_2O species gives rise to an IR band at 2250–2150 cm^{-1}.

A number of schemes have been proposed to convert NO to nitrogen and oxygen. Recent work by Spoto *et al.* (18) led to the reaction scheme outlined in Fig. 23, which agreed with work by Giamello *et al.* (22). This scheme suggests that conversion of NO to N_2 and O_2, starts by adsorption of NO onto Cu^+ sites, forming mono- and dinitrosyl species (structures I and II), which subsequently convert to structure III (unstable Cu complex with N_2O and O^- adsorbed species). Liberation of N_2O leads to structure (IV)–a Cu^{2+} species characterized by an IR band at 1900 cm^{-1}. The reactive O^- atom reacted with a further NO molecule to give a ON–Cu^{2+}–NO_2^- species with IR bands at 1630–1600 cm^{-1} (structure V)) which have been postulated as the reactive intermediates in NO decomposition (17, 21). Cu^+ sites are regenerated by decomposition of the above complex to oxygen and nitrogen and desorption of oxygen at higher temperatures.

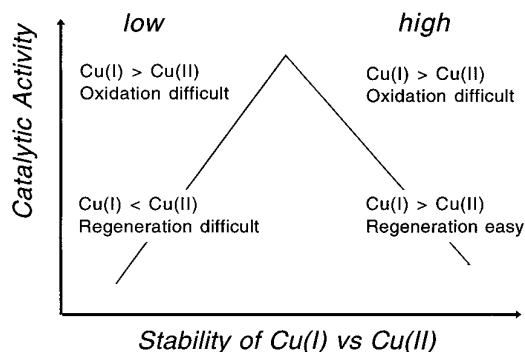The catalytic performance of Cu in a zeolite matrix for

FIG. 24. Catalytic activity chart.

the decomposition of NO is linked to the $Cu^+ \leftrightarrow Cu^{2+}$ redox cycle which is essential for the formation of the ON–Cu^{2+}–NO_2^- complex, and thus dependent on the relative stability of the Cu(I) and Cu(II) species. The desirable stability of Cu(I) sites for a good catalyst lies in a optimum range (Fig. 24). In this range, the rate of oxidation of Cu(I) to Cu(II) is fast, while the concentration of recovered Cu(I) sites from desorption remains high. On the other hand, if the stability of Cu(I) was low, regeneration of Cu(I) sites was difficult. If the stability of Cu(I) was very high, then oxidation to Cu(II) would not occur easily.

In Cu–UHSY and Cu–mordenite, the oxidation of Cu(I) to Cu(II) by NO was low, as supported by a very weak 2250–2150-cm^{-1} band. All the nitrosyl bands were observed to increase in intensity with increasing NO pressure. This simultaneous growth of the 1900, 1810, and 1730-cm^{-1} bands suggested that Cu(II) and Cu(I) sites were being filled, and at high NO partial pressures some dinitrosyl species formed.

Over-exchanged Cu–ZSM5 catalyst is a superior catalyst due to the following properties:

(i) The stability of the catalytic Cu(I) sites;

(ii) The oxidation of Cu(I) to Cu(II) according to the reaction scheme (Fig. 23) at acceptable rates;

(iii) The facile regeneration of active sites.

In summary, the redox chemistry of Cu sites in over-exchanged ZSM5 was well matched to the NO decomposition mechanism. In other zeolite matrices, Cu(II) is too stable (for example Cu–M-57). This allowed high oxidation rate, but regeneration of Cu(I) sites became difficult, thus the reaction ceased after the first cycle. In other cases, Cu(I) was very stable (for example Cu–UHSY-165) and oxidation to Cu(II) via the reaction scheme (Fig. 23) was unfavorable.

REFERENCES

1. Saito, K., and Ichihara, I., *Catal. Today* **10,** 45 (1991).
2. Armor, N. J., *Appl. Catal. B: Environ.* **1,** 221 (1992).
3. Taylor, C. K., *Catal. Rev. Sci. Eng.* **35**(1), 457 (1993).

4. Airnazmi, A., Benson, E. J., and Boudart, M., *J. Catal.* **30,** 55 (1973).

5. Winter, R. S. E., *J. Catal.* **22,** 158 (1971).

6. Teraoka, Y., Yoshimatsu, M., Yamazoe, N., and Seiyame, T., *Chem. Lett.* 893 (1984).

7. Shin, S., Ogawa, K., and Shimomura, K., *Mater. Res. Bull.* **14,** 133 (1979).

8. Uchijima, T., *Hyomen* **18,** 132 (1980).

9. Iwamoto, M., Yahiro, H., Mine, Y., and Kagawa, S., *Chem. Lett.* 213 (1989).

10. Herreros, B., Man, P. P., Manoli, J. M., and Fraissard, J., *J. Chem. Soc. Chem. Commun.* 464 (1992).

11. Iwamoto, M., Yahiro, H., Tanda, K., Mizuno, N., Mine, N., and Kagawa, S., *J. Phys. Chem.* **95,** 3727 (1991).

12. Li, Y., and Armor, N. J., *Appl. Catal.* **76,** L1 (1991).

13. Iwamoto, M., Yahiro, H., Mizuno, N., Zhang, X. W., Mine, Y., Furukawa, H., and Kagawa, S., *J. Phys. Chem.* **96,** 8360 (1992).

14. Iwamoto, M., Yookoo, S., Sakai, R., and Kagawa, S., *J. Chem. Soc. Faraday Trans 1* **77,** 1629 (1981).

15. Li, Y., and Hall, W. K., *J. Catal.* **129,** 202 (1991).

16. Li, Y., and Hall, W. K., *J. Phys. Chem.* **94,** 16 (1990).

17. Spoto, F., Bordiga, S., Scarano, D., and Zecchina, A., *Catal. Lett* **13,** 39 (1992).

18. Spoto, G., Zecchina, A., Bordiga, S., Richiardi, G., and Mata, G., *Appl. Catal. B: Environ.* **3,** 151 (1994).

19. Ebitani, K., Morokuma, M., Kim, H. J., and Morikawa, A., *J. Catal.* **141,** 725 (1993).

20. Valyon, J., and Hall, W. K., *J. Catal.* **143,** 520 (1993).

21. Valyon, J., and Hall, W. K., *J. Phys. Chem.* **97,** 1204 (1993).

22. Giamello, E., Murphy, D., Magnacca, G., Morterra, C., Shioya, Y., Nomura, T., and Anpo, M., *J. Catal.* **136,** 510 (1992).

23. Petunchi, O. J., Marcelin, F., and Hall, W. K., *J. Phys. Chem.* **96,** 9967 (1992).

24. Guilloiry, A. W., and Hunter, E. C., *J. Chem. Phys.* **50,** 3516 (1969).

25. Anpo, M., Matsuoka, M., Shioya, Y., Yamashita, H., Giamello, E., Morterra, C., Che, M., Patterson, H. H., Webber, S., Ouellette, S., and Fox, A. M., *J. Phys. Chem.* **98,** 5744 (1994).

26. Chao, C. C., and Lunsford, H. J., *J. Phys. Chem.* **76**(11), 1546 (1972).

27. Mabilon, G., and Durand, D., *Catal. Today* **17,** 285 (1993).